Pulse Oximeter with Digital Readout of SpO_2 and Heart Rate

Alex Lu
Department of Bioengineering
University of San Diego, California

Longyu Zhang
Department of Bioengineering
University of San Diego, California

Eeman Iqbal
Department of Electrical Engineering
University of San Diego, California

Taiming Chen
Department of Bioengineering
University of San Diego, California

***Abstract*—Obstructive sleep apnea (OSA) is a disorder that affects blood oxygen saturation levels. Untreated OSA often leads to metabolic, cardiovascular, and neurocognitive morbidities. A portable overnight pulse oximeter, which monitors the change in blood oxygen level, is often used as a practical screening tool in primary care settings. This project study focuses on designing a pulse oximeter that measures SpO_2 and heart rate. The setup primarily covers two flashing LEDs, a signal differentiation system, filtering circuits, and Arduino hardware. The project design includes receiving light signals from LEDs and filtering them and finally processing them using Arduino. By comparing absorbances of light signals from two different wavelengths, the blood oxygen level can be successfully calculated and displayed on the pulse oximeter.**

I. INTRODUCTION

Obstructive sleep apnea (OSA) is a very common sleep-related disorder that affects approximately 15 to 30 of males and 10 to 15 percent of females in North America [1]. The main characteristic of OSA is recurring episodes of partial or complete blockage of the upper airway during sleep due to the relaxation of muscles in the back of the throat. Long-term OSA often leads to many health problems such as high blood pressure, type 2 diabetes, and daytime fatigue. Further, Sleep Apnea has been found to be strongly associated with heart failure, with up to 40% prevalence in heart failure patients [2]. Therefore, it is essential to facilitate early diagnosis of the condition. However, OSA has been proven to be highly prevalent but underdiagnosed [3], [4]. Possible explanations for underdiagnoses include a lack of awareness of the signs and symptoms, limited access to diagnostic tools that are often in labs or hospitals, and negative stigma behind OSA relating to obesity and snoring.

OSA is known to cause repeated episodes of hypoxemia and increases in heart rate and blood pressure throughout the night [2]. Hypoxemia is characterized by low oxygen levels in the blood. While a normal healthy oxygen level in the blood is above 95%, it is difficult to visually identify hypoxemia unless the oxygen level drops below 80% [5]. Indeed, hypoxemia is not only related to OSA. A low blood oxygen level can also be an indicator of various disorders such as asthma, COVID-19, and pneumonia. Therefore, it is critical to provide an efficient method for detecting oxygen levels in the blood.

The introduction of pulse oximetry has revolutionized the way medical professionals monitor the blood oxygen levels of affected patients. Pulse oximetry is a non-invasive monitoring method that takes advantage of the light absorbance of oxygenated and deoxygenated blood to monitor blood oxygen levels. Various studies have proven the effectiveness of pulse oximetry for OSA. Noting that early confirmation and treatment of OSA could greatly prevent further complications [6], pulse oximetry has proven to be effective in identifying patients with OSA, with the ability to identify the severity of OSA in more than 80% of cases [7].

In this paper, we propose a circuit design for the implementation of pulse oximetry and analyze the design through Falstad circuit simulation.

II. PHYSIOLOGY

Prior to developing a system for measuring oxygen saturation levels and heart rate, it is important to understand where these metrics are present in the human body and how they can be measured.

A. Blood Oxygen Saturation

Oxygen Saturation is the ratio of oxygen-saturated hemoglobin to the total amount of hemoglobin in the blood, measured using oxyhemoglobin (HbO_2) and reduced hemoglobin (Hb), indicators of oxygen within arterial blood.

$$SaO_2 = \frac{C_{HbO_2}}{C_{HbO_2}+C_{Hb}} \quad (1)$$

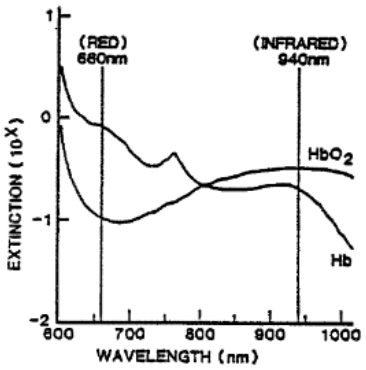

Fig. 1. The absorbance of light by reduced hemoglobin (Hb) and oxyhemoglobin (HbO_2) at 660 nm (red) and 940 mm (infrared) [8]

HbO_2 and Hb have different absorption spectra, with the extinction coefficient of HbO_2 being higher than Hb at an infrared (IR) wavelength and the reverse true at the wavelength of red light. As shown by (Fig. 1), the reversal of spectral absorptivity characteristics across different wavelengths indicates an isosbestic wavelength, at which HbO_2 and Hb have the same absorbance. While total absorbance is usually found using Beer's Law (Eq. 2), this connection allows for the pulse oximeter to estimate arterial blood saturation (SpO_2) using the ratiometric technique.

$$A(\lambda) = W \cdot L \cdot \alpha(\lambda) \quad (2)$$

In (Eq. 2), W is the molar density of a material, L is the optical path length, and $\alpha(\lambda)$ is the absorptivity at a particular wavelength.

Light absorption in tissue includes absorption due to tissue, venous blood, and arterial blood. Most of these remain constant over time; however, the absorption of arterial blood varies with its volume, which changes in response to pulse rate [10]. By defining the varying absorption of arterial blood by volume as an AC signal, and the remaining constant parts of tissue absorption as the DC signal, the AC signal can then be divided by the DC signal to scale it (Fig. 2).

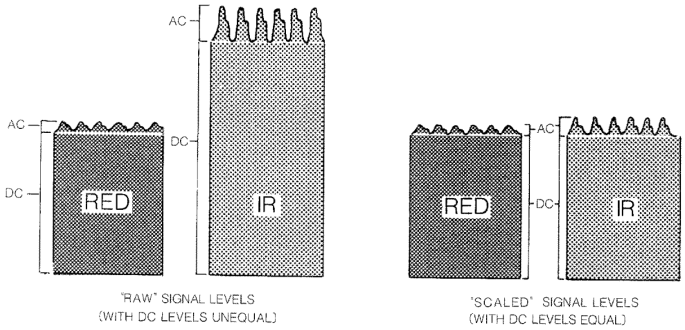

Fig. 2. Graphical representation of the compensation needed to utilize light intensities at two wavelengths for calculation. [8]

Once the AC/DC signals have been found for both red and IR wavelengths, their ratio (Eq. 3) can be used to calculate SpO_2 (Eq. 4).

$$R = \frac{\frac{AC(\lambda_{RED})}{DC(\lambda_{RED})}}{\frac{AC(\lambda_{IR})}{DC(\lambda_{IR})}} \quad (3)$$

$$SpO_2 = 110 - 25R \quad (4)$$

B. *Heart rate*

Measuring the volume variations in the blood (or pulse rate) using IR light is referred to as photoplethysmography (PPG). The AC signal from shining infrared light into tissue is also a PPG signal (Fig. 3), and can be used to find heart rate. As heart rate measures the number of contractions per minute, it corresponds to the variation in arterial blood volume.

$$HR = \frac{60}{T_{pp}} \quad (5)$$

Eq. (5) shows how the heart rate can be found by measuring the time in between peaks (or heart contractions) per minute. T_{pp} is the time between peaks.

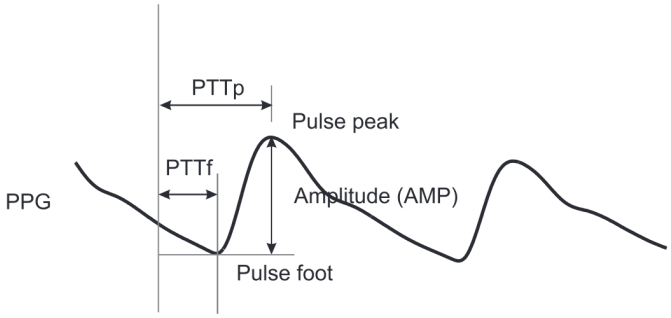

Fig. 3. Single-site PPG waveforms with key properties labeled [9]

III. CIRCUIT DESIGN

The full design is based on transmission pulse oximetry, as its accuracy is much better than that of reflection pulse oximetry.

(Fig. 4) is a block diagram of all components in the circuit. An alternating LED activator outputs two voltage signals, V_{IR} and V_{RED}, which control their respective IR and red LED lights. The light from the LEDs is shined into a finger, transmitting a signal through tissue. Both transmitted signals are then picked up by a single photodiode, creating a current signal, and run through a transimpedance amplifier to get voltage output V_{Photo}. This signal is split into two outputs, IR_{Signal} and Red_{Signal}, using a Dual Sample and Hold Switch. The two signals are then separately run through a series of low-pass filters (to remove noise and get the DC component) and high-pass filters (to remove the DC offset and get the AC component). The DC and AC component values are read into an Arduino, which calculates SpO_2 and heart rate, outputting the results on a digital display.

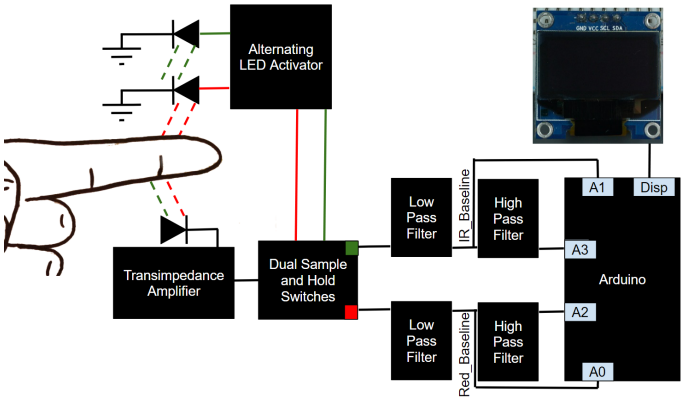

Fig.4. An overview of the entire circuit design.

A. *Alternating LED Activator*

The Alternating LED Activator in (Fig. 5) allows for the alternating activation of the red LED light and the infrared LED light and sends out V_{Red}, and V_{IR} as control signals for reading red and infrared intensities later in the circuit.

The first component is a 555 timer set up as an astable oscillator powered by a 5V power supply, as displayed in Fig. 5a. The charge time of the system is set to 1ms using the below equation:

$$T = 0.7RC = 0.001\ second \quad (6)$$

With R = 4.7kΩ and C = 395nF. In order to generate a 50% duty cycle, a diode is used to connect the discharge to the threshold of the 555 timers. The 50% duty cycle astable oscillator generates a signal that alternates between 0V and 5V every 1 ms. This signal is then split into two, with one side connected to an inverter displayed in Fig. 5b. This way, as the signal alternates, when one side is on, the other side will be off and vice versa, creating an alternating signal.

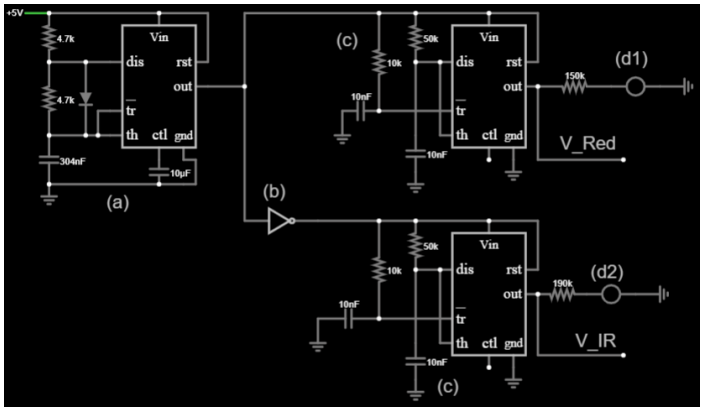

Fig. 5. A circuit diagram of the Alternating LED Activator

When operating LED lights, it is important to ensure the LED lights are not left on for too long to prevent overheating and reduce power consumption. For this reason, a 555 timer set up as a monostable oscillator is connected to each of the outputs of the astable oscillator, as displayed in Fig. 5c. The charge time of the monostable oscillator is set to 0.5ms using the equation below:

$$T = 1.1RC = 0.0005\,seconds \tag{7}$$

With R = 50kΩ and C = 10nF. The monostable oscillator combined with the astable oscillators allows for an overall 25% duty cycle. The LED lights will be off for longer periods of time, reducing heat exerted and power consumed.

The output of the monostable oscillators is connected to the LED resistor in series with the LED light. Common red LED lights have an operating forward voltage of 2V and forward current of 20 uA [10], and common infrared LED lights have an operating forward voltage of 1.2V and forward current of 20uA [11]. Utilizing the following equation:

$$R_{LED} = \frac{V_{supply} - V_{forward}}{I_{forward}} \tag{8}$$

The red LED resistor is set to 150kΩ (Fig. 5d1) and the infrared LED resistor is set to 190kΩ (Fig. 5d2). Further, before the resistor, the voltage signal is split off as V_{Red} and V_{IR} to be used as control signals for the dual sample and switch.

B. *Transimpedance Amplifier*

The photodiode receives the transmitted signals from both LEDs and outputs a current between 0 and 70 µA [12]. A transimpedance amplifier, as designed in (Fig. 6), was used to convert the current output to a voltage signal, to be used in the rest of the circuit.

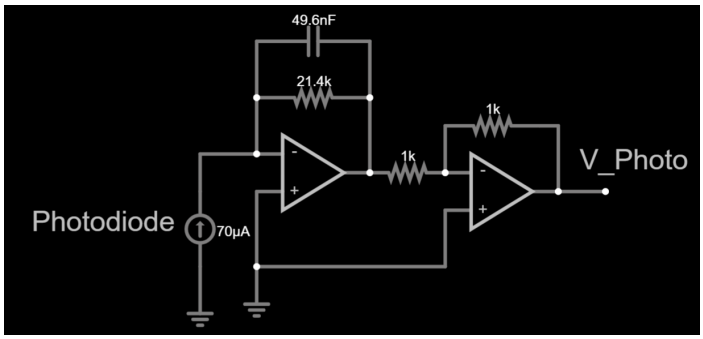

Fig 6. A circuit diagram of the transimpedance amplifier.

For this circuit design, it is ideal for the voltage output to be between 0 to 1.5V. In order to achieve this, the transimpedance amplifier must include a set gain of 21400. The relationship between V and I is given in the below equations:

$$\frac{V_{photo}}{I_{Photo}} = -Z_{top} \tag{9}$$

$$Z_{top} = Z_C || Z_R = \frac{R}{jwRC+1} \tag{10}$$

Where Z_{top} is the impedance across the top side of the circuit. The gain is directly related to the value of R. Therefore R is set to 21.4kΩ. In addition to the gain, doing some initial filtering of the current signal is preferable. Here the cut-off frequency is given in the equation below:

$$f_c = \frac{1}{2\pi RC} \tag{11}$$

Aiming for a low pass noise filtering cut-off frequency of 150Hz with R set to 21.4kΩ, the C is set to 49.6nF.

An inverting amplifier with a gain of 1 is appended to the output of the transimpedance amplifier to ensure the voltage signal remains positive.

C. *Dual Sample and Hold Switch*

Because the same photodiode was used to receive the transmitted signals from both red and IR LEDs, a pair of sample and hold switches, set up as in (Fig. 7), are implemented to differentiate between them for the sake of analysis and calculations.

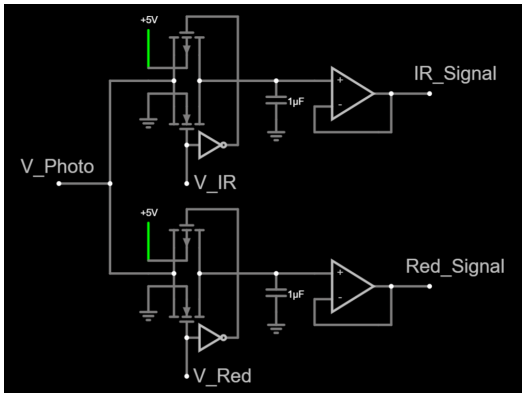

Fig. 7. A circuit diagram of the Dual Sample and Hold Switch

Both switches consist of an n-type MOSFET (NMOS) and p-type MOSFET (PMOS) connected in parallel. Their sources are tied to the output of the transimpedance amplifier, V_{Photo}, while their drains are connected to a capacitor and buffer (unity gain Op-Amp). Both NMOS transistors have their body tied to the ground; both PMOS transistors likewise have their body tied to the input voltage from the battery.

As shown in (Fig. 7), the top switch has the gate of its NMOS transistor connected to V_{IR} from the Alternating LED Activator. The gate of its PMOS transistor is connected to the inverted V_{IR} signal. Correspondingly, for the bottom switch, the gates of the NMOS and PMOS transistors are respectively connected to V_{RED} and its inverted signal.

When the signals for either V_{IR} or V_{RED} are high, the corresponding switch "turns on" and current is allowed to flow across the MOSFETS. The capacitor will charge or discharge as necessary to allow the output of the switch (IR_{Signal} and Red_{Signal}) to match the voltage of the photodiode (V_{Photo}). When the relevant V_{IR} or V_{RED} signal is low, the switch "turns off" and the capacitor stores the voltage until the switch turns back on.

Both capacitors have a capacitance of 1 µF, low for the purposes of faster charging, but high enough to prevent leak. The transistors all have the base properties of a MOSFET on Falstad, with threshold voltages $|V_{tp}| = V_{tn} = 1.5$ V.

D. Low Pass Filter

In order to remove unwanted noise, the IR_{Signal} and Red_{Signal} are both run through a 4th-order Butterworth filter, displayed in (Fig.8). The Butterworth filter has a maximally flat frequency response, without introducing any ripples or distortions in the passband. In addition, a 4th-order filter provides a steeper roll-off than a 2nd-order filter, meaning that it can attenuate frequencies outside the passband more effectively. This is important for removing any high-frequency noise that may have been introduced during the signal acquisition process.

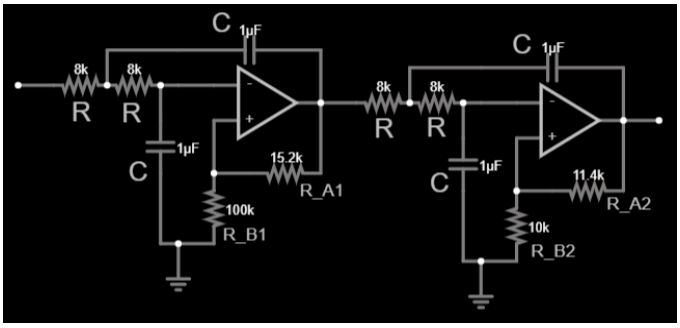

Fig. 8. A circuit diagram of the low pass filter

In this case, a 4th-order Butterworth filter is constructed by connecting two 2nd-order filters in a cascade arrangement. To achieve the most uniform response for a 4th-order filter, it's essential to use distinct voltage gains for both stages rather than the maximum flat response of 1.586 typically associated with a 2nd-order Butterworth filter. Based on the information provided in Figure 9, the ideal voltage gains for the first and second stages are 1.152 and 2.235, respectively, which results in the maximum flat response for the 4th-order Butterworth filter [15].

Poles	Butterworth (DC Gain H_0)	Chebyshev (0.5dB) λ_n	Chebyshev (0.5dB) Gain	Chebyshev (2.0dB) λ_n	Chebyshev (2.0dB) Gain
2	1.586	1.231	1.842	0.907	2.114
4	1.152	0.597	1.582	0.471	1.924
	2.235	1.031	2.660	0.964	2.782
6	1.068	0.396	1.537	0.316	1.891
	1.586	0.768	2.448	0.730	2.648
	2.483	1.011	2.846	0.983	2.904
8	1.038	0.297	1.522	0.238	1.879
	1.337	0.599	2.379	0.572	2.605
	1.889	0.861	2.711	0.842	2.821
	2.610	1.006	2.913	0.990	2.946

Fig. 9. Sallen-Key low pass filter characteristic gains [13]

This could then be used to calculate the component values for the gain of both stages, which depend on R_A and R_B (Eq. 12).

$$Gain = 1 + \frac{R_A}{R_B} \tag{12}$$

The low pass filter also uses a cutoff frequency of 20 Hz, chosen to remove unwanted high-frequency noise while retaining the low-frequency DC component of the signal [14], which is important for accurate measurement of oxygen saturation levels in the blood. The 4th order Butterworth filter transfer function (Eq. 13) and cutoff frequency (Eq. 14) were then used to find the values of resistors and capacitors used in both stages, R = 8 kΩ and C = 1 µF

$$H(s) = H_1(s) \cdot H_2(s) \tag{13}$$
$$= \frac{1.152}{(sRC)^2+1.848sRC+1} \cdot \frac{2.235}{(sRC)^2+0.765sRC+1}$$
$$= \frac{2.5747}{(sRC)^4+2.6131\,(sRC)^3+3.4142(sRC)^2+2.6131(sRC)+1}$$

$$f_c = \frac{1}{2\pi RC} = 19.89\ Hz \tag{14}$$

The Bode plots shown in (Fig. 10) confirm the component values chosen.

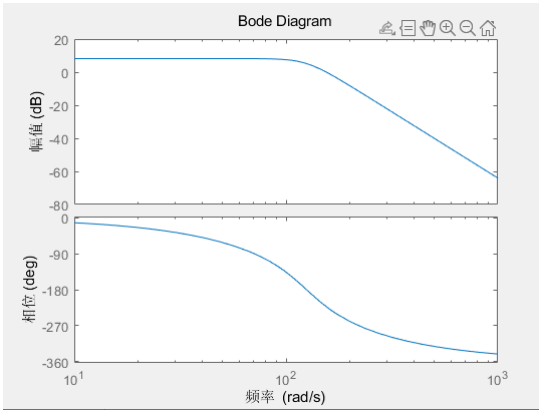

Fig. 10. Bode Diagram of the low pass filter, showcasing amplitude changes in dB and phase changes in degrees versus frequency in rads/s. Gain reaches 0 as frequency goes above ~100 rad/s.

E. High Pass Filter

The output of each low pass filter is inputted into a high pass filter (Fig. 11). The goal of the high pass filter is to obtain the AC component of the signals received from the photodiode by filtering out the DC offset after the noise has been removed using the low pass filter.

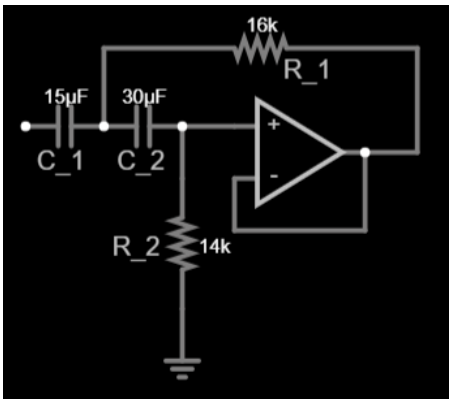

Fig. 11. A circuit diagram of the high pass filter

Here, a 2nd-order filter was chosen due to providing a steeper roll-off than 1st order, for more effective removal of the signal's DC component while minimizing attenuation of the AC signal. The transfer function is shown in (Eq. 15).

$$\frac{V_{out}(s)}{V_{in}(s)} = \frac{s^2}{s^2+s(\frac{1}{R_2C_1}+\frac{1}{R_2C_2})+\frac{1}{R_1C_1R_2C_2}} = \frac{s^2}{s^2+7.1429s+9.9206} \quad (15)$$

The cutoff frequency was chosen to be at least 0.5 Hz to remove the DC offset [14]. As confirmed in (Eq. 16), the component values were chosen to be R_1 = 16 kΩ, R_2 = 14 kΩ, C_1 = 15 µF, and C_2 = 30 µF

$$f_c = \frac{1}{2\pi\sqrt{R_1C_1R_2C_2}} = 0.501\ Hz \quad (16)$$

Correspondingly, the Bode plots for the high pass filter are shown in (Fig. 12).

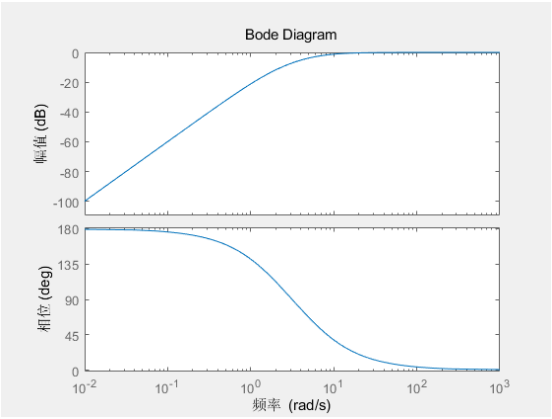

Fig. 12. Bode Diagram of the high pass filter, showcasing amplitude changes in dB and phase changes in degrees versus frequency in rads/s. Gain reaches 0 as frequency goes below ~1 rad/s

F. *Arduino Integration*

The outputs of the low pass filters (DC_{IR} and DC_{RED}) and high pass filters (AC_{IR} and AC_{RED}) are read into an Arduino controller, which calculates the SpO_2 and BPM, displaying the results on an OLED display.

While the main equations have been previously listed in Section II, the code also includes a function to find the peaks of a signal, used in calculating the heart rate.

The full Arduino code is in the Appendix.

IV. RESULTS

In order to validate the design of the circuit, each individual component of the circuit is tested using Falstad simulations software. This way, the function of each circuit component can be compared with the expectation set. The complete circuit will also be analyzed by testing a simulated V_{Photo} signal.

A. *Alternating LED Activator*

To validate the Alternating LED Activator, the 555 timers are connected to 5V voltage supplied, and their outputs for V_{Red} and V_{IR} are plotted in (Fig. 13).

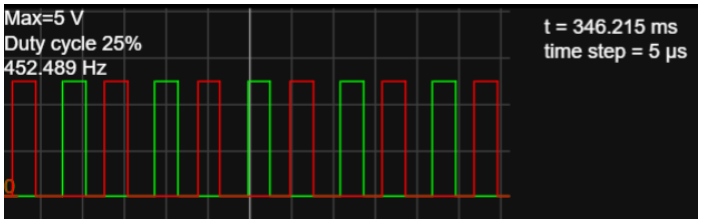

Fig. 13. V_{Red} (red) and V_{IR} (green) of the Alternating LED Activator with 5V power supply.

The circuit component successfully outputs alternating signal waves in a 25% duty cycle, allowing for the generation of control signals and activation of LED lights. However, the frequencies are not perfectly 500Hz. This could be attributed to the limitations of capacitors with possible leakages and variations in charge time. Though this frequency variation will not cause a large problem for the overall instrument as both the LED lights and the Dual Sample and Hold Switch are controlled by the same signal.

B. *Transimpedance Amplifier*

To test the transimpedance amplifier, a current running from 0 - 70 uA is simulated in place of the photodiode. The output voltage is recorded and plotted against the input current to analyze current and voltage relations.

As seen in (Fig 14), the output voltage corresponds directly with the input current, and the peak voltage and current confirm the voltage gain of 21400.

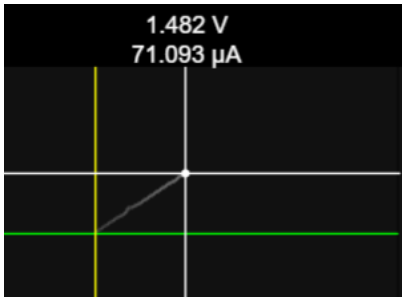

Fig. 14. The voltage output (yellow) is plotted against the input current (green). The rough maximum value is shown.

C. *Dual Sample and Hold Switch*

To test the Dual Sample and Hold Switch, an input V_{Photo} is simulated as two intertwined waves of 7 Hz frequency with 180° offset sampled at 500Hz, 25% duty cycle. V_{Photo} simulates the response to light intensities as the red and infrared

lights are turned on and off. The switches are linked to a simulated alternating control signal of 500 Hz 25% duty cycle.

As seen in (Fig 15), the Dual Sample and Hold Switch effectively separate the sampling voltage signal of V_{Photo} into two distinct waves. While these results are expected, the simulated input is also in an ideal scenario. There could be cases where the sample and hold happened to hold a signal amplitude that is part of some noise, which could affect the accuracy of the output signals.

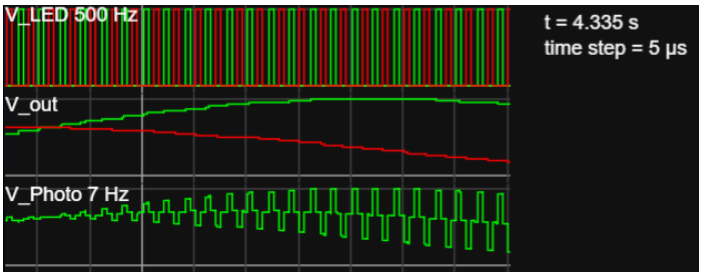

Fig. 15. The input V_{Photo} (bottom green) into the Dual Sample and Hold Switch is displayed at the bottom. V_{LED} indicates the control signals of the switches: V_{Red} (top red) and V_{IR} (top green). V_{out} is the output signals: Red_{Signal} (middle red) and IR_{Signal} (middle green)

D. *Low Pass Filter*

As seen in red in (Fig. 16), the low pass filter effectively allows frequencies below 20 Hz to pass. Above 20 Hz, the amplitude of the signal gradually declines to zero at around 60 Hz. Indeed, the low pass filter does not perfectly cut out frequencies above 20 Hz, but this is the inherent shortcoming of filters in realistic scenarios. The 4th-order Butterworth filter is implemented to improve this cut-off effectiveness.

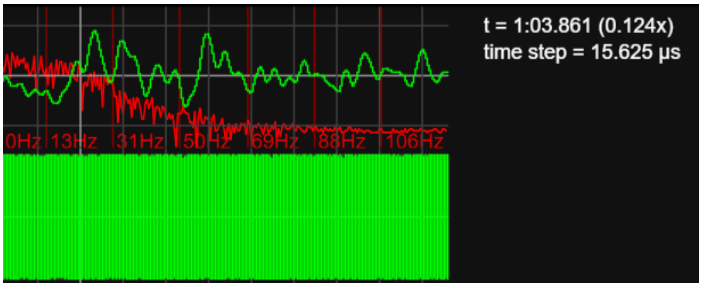

Fig. 16. This figure shows the noise input (bottom green) and filtered output (top green), along with the frequency range (top red) of the low pass filter in Falstad.

E. *High Pass Filter*

To test the high pass filter, 3 different waves are passed through the circuit component in order to examine the output.

As shown in (Fig. 17), the high pass filter successfully removes the DC components of the waves while maintaining the wave shape. Although upon closer inspection, there are some minor variations in DC offsets (non-zero) and wave amplitude of the output waves. The DC offset error could lead to calculation error for SpO2, and is likely attributed to the imperfect frequency cutoff for these types of circuits like what happened for the low pass filter.

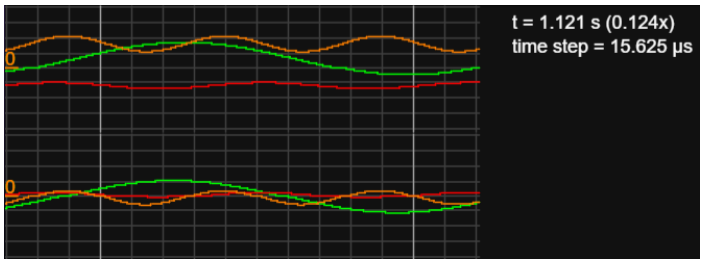

Fig. 17. High pass filter input signals displayed at the top are compared to output signals displayed at the bottom. The waves are 1) 2.5V amplitude wave with 8 DC offset at 20 Hz frequency and 167 degrees offset (orange), 2) 5.5V amplitude wave with 3 DC offset at 7Hz frequency and 23 degrees offset (green), and 3) 1.0V amplitude wave with -6 DC offset at 15 Hz frequency and 890 degrees offset (red).

F. *Combined Circuit Analysis*

To complete the results section, all circuits are combined, and a simulated V_{Photo} is applied as input for the Dual Sample and Hold Switch. V_{Photo} is a combination of 1) a 0-1.5V wave with 15 Hz frequency and 0-degree offset and 2) a 0-1.5V wave with 12 Hz frequency and 176-degree offset.

As seen in (Fig. 18), the Dual Sample and Hold Switch successfully samples the wave with high accuracy, splitting the signal into red and infrared signals. V_{LPF} shows that the wave is successfully filtered of high-frequency portions through the low pass filter, leaving a smooth wave with some phase shift. V_{LPF_HPF} indicates that the high pass filter filtered out the DC offset, leaving only the AC component centered at 0 offsets. Notably, the V_{LPF} will be used as the DC baseline in Arduino and V_{LPF_HPF} will be the AC component for the Arduino.

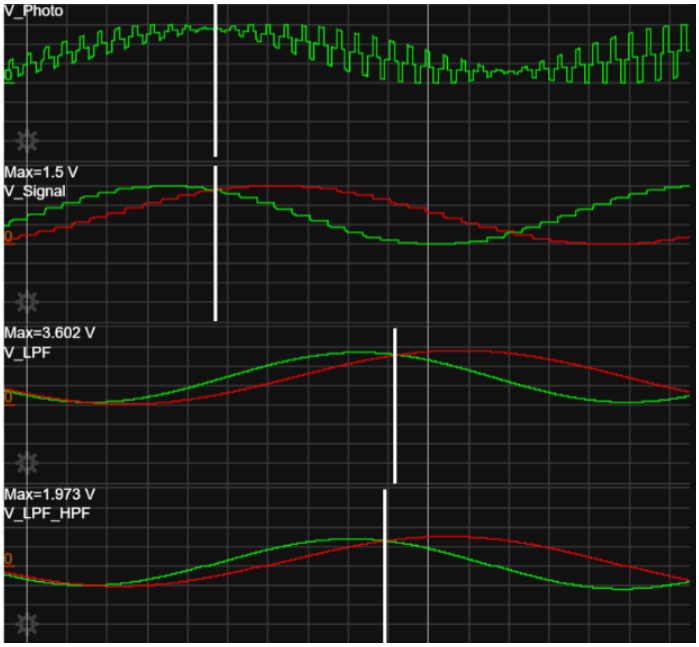

Fig. 18. V_{Photo}, V_{Signal} after Dual Sample and Hold Switch, V_{LPF} after the low pass filter, and V_{LPF_HPF} after the high pass filter plotted in the same time domain. For V_{Signal}, V_{LPF}, and V_{LPF_HPF}, red represents the red LED signal, and green represents the infrared LED signal. The white horizontal line indicates a phase shift between stages.

V. CONCLUSION

The main advantages of this design of pulse oximeter includes its non-invasiveness that enables for painless and risk-free measurements, as well as relatively accurate readings in comparison with many commercial devices. These encourage

patients to constantly monitor their physiological parameters such as SpO2 with confidence. The design also makes measurements of these parameters more convenient. The use of LEDs and photodiodes offers a simple but effective method for capturing these vital signs. There are several limitations in the current design as well. Due to the movement of the measured subject during the measuring session, motion artifacts are likely to introduce inaccuracies in the readings. The accuracy of the device will also be affected by ambient light interference since it could lead the photodiode to sense external light sources. Various skin pigmentation differences of users could lead to different degrees of light absorption, which could also impact the accuracy of SpO2 readings. In addition, poor contact between the sensor and the skin could also result in inconsistent readings.

In conclusion, the pulse oximeter design demonstrates the potential in providing accurate and convenient measurements of SPO2 and heart rate. To overcome the limitations identified, future improvements should focus on incorporating motion artifact reduction techniques, such as adaptive filtering algorithms, to minimize the impact of movement on the readings. Shielding the device from ambient light or implementing an additional channel for measuring ambient light could help mitigate interference from external light sources. Or incorporating an extra channel for ambient light voltage in the sample and holding switches stage for common mode suppression. Calibration methods that take into account skin pigmentation differences should also be considered to enhance the accuracy of SPO2 measurements across diverse populations. Improving the topology of the device and sensor design for better skin contact can lead to more consistent and reliable readings. Furthermore, optimizing the device to reduce power consumption and using techniques such as duty cycling or power management algorithms will improve battery life and overall usability. Essentially, more testing and validation using real components and diverse populations should be conducted to ensure the device's performance in real-world scenarios. By addressing these limitations and implementing the suggested improvements, the pulse oximeter can become a valuable tool for monitoring blood oxygen levels and heart rate in various medical and non-medical applications.

ACKNOWLEDGEMENTS

We appreciate Dr. Gert Cauwenberghs for his lectures on bioinstrumentation. The team finds BENG 186B lecture materials highly practical and beneficial for a future in designing and constructing medical devices and instruments. We also appreciate Samira Sebt, Vikrant Jaltare, and Adyant Balaji for their continued guidance throughout BENG 186B Winter 2023 at the University of California, San Diego.

REFERENCES

[1] Kline, L. R. (2022, June 1). Clinical presentation and diagnosis of obstructive sleep apnea in adults. In N. Collop (Ed.). UpToDate.

[2] Gottlieb, J. D. *et al.*, “Hypoxia, Not the Frequency of Sleep Apnea, Induces Acute Hemodynamic Stress in Patients with Chronic Heart Failure,” *J Am Coll Cardiol*, vol. 54, no. 18, pp. 1706–1712, Oct. 2009, doi: 10.1016/j.jacc.2009.08.016.

[3] Fuhrman, Claire, et al. "Symptoms of sleep apnea syndrome: high prevalence and underdiagnosis in the French population." Sleep medicine 13.7 (2012): 852-858.

[4] Loo, Guo Hou, et al. "Prevalence of obstructive sleep apnea in an Asian bariatric population: an underdiagnosed dilemma." Surgery for Obesity and Related Diseases 16.6 (2020): 778-783.

[5] Jubran, A. “Pulse oximetry,” *Crit Care*, vol. 3, no. 2, pp. R11–R17, 1999, doi: 10.1186/cc341.

[6] Chiang, L.-K. “Overnight pulse oximetry for obstructive sleep apnea screening among patients with snoring in primary care setting: Clinical case report,” *J Family Med Prim Care*, vol. 7, no. 5, pp. 1086–1089, 2018, doi: 10.4103/jfmpc.jfmpc_142_18.

[7] Rosa, João Carlos Fraga da et al. “Diagnostic accuracy of oximetry for obstructive sleep apnea: a study on older adults in a home setting.” Clinics (Sao Paulo, Brazil) vol. 76 e3056. 1 Oct. 2021, doi:10.6061/clinics/2021/e3056

[8] Wukitsch, M. W., Petterson, M. T., Tobler, D. R.and Pologe, J. A. “Pulse oximetry: Analysis of theory, technology, and practice,” *J Clin Monitor Comput*, vol. 4, no. 4, pp. 290–301, Oct. 1988, doi: 10.1007/BF01617328.

[9] Allen, J. “Quantifying the Delays Between Multi-Site Photoplethysmography Pulse and Electrocardiogram R-R Interval Changes Under Slow-Paced Breathing,” *Frontiers in Physiology*, vol. 10, 2019, Accessed: Mar. 23, 2023. [Online]. Available: https://www.frontiersin.org/articles/10.3389/fphys.2019.01190.

[10] “LED - Basic Red 5mm - COM-09590 - SparkFun Electronics.” https://www.sparkfun.com/products/9590 (accessed Mar. 23, 2023).

[11] “How IR LED Voltage Drop Effects LED Performance and Life Cycle,” Dec. 04, 2019. https://resources.pcb.cadence.com/blog/2019-how-ir-led-voltage-drop-effects-led-performance-and-life-cycle (accessed Mar. 23, 2023).

[12] Duun, S., Haahr, R. G., Birkelund, K., Raahauge, P., Petersen, P., Dam, H., Noergaard, L., & Thomsen, E. V. (2007). A Novel Ring Shaped Photodiode for Reflectance Pulse Oximetry in Wireless Applications. In Proceeedings of the 6th IEEE Conference on Sensors (pp. 596-599). IEEE. https://doi.org/10.1109/ICSENS.2007.4388469(accessed Mar. 23, 2023).

[13] “butterworth filter design,” *studylib.net*. https://studylib.net/doc/18656787/butterworth-filter-design

[14] Shimizu, T., Hatano, Y., and Shimoyama, H. "Design and control of a pneumatically actuated origami-inspired robot," AIP Advances 2, 042187 (2012); DOI: 10.1063/1.4759491.

[15] Electrical4u, "Butterworth Filter," Electrical4u.com. Available: https://www.electrical4u.com/butterworth-filter/. Accessed on: Mar. 22, 2023.

APPENDIX

```
#include <Wire.h>
#include <Adafruit_SSD1306.h>

#define OLED_RESET 4
Adafruit_SSD1306 display(OLED_RESET);

const int redDCPin = A0; // Analog input pin for DC signal from red LED
const int irDCPin = A1; // Analog input pin for DC signal from IR LED
const int redACPin = A2; // Analog input pin for AC signal from red LED
const int irACPin = A3; // Analog input pin for AC signal from IR LED

const int numSamples = 1000; // Number of samples to average for each reading

// Function to find the time between peaks in the given signal
float findPeakTime(int signalPin) {
  int threshold = 512; // Threshold for peak detection
  int peakCount = 0; // Count of peaks found
  float lastValue = analogRead(signalPin); // Last value of the signal
  float peakTime = 0.0; // Time of the last peak found
  float sampleRate = 1000.0 / numSamples; // Sample rate in Hz

  // Iterate over the samples in the signal
  for (int i = 0; i < numSamples; i++) {
              float value = analogRead(signalPin);
              if (lastValue < threshold && value >= threshold) {
              // A peak has been found
              if (peakCount == 0) {
              // This is the first peak found
              peakTime = i * (1.0 / sampleRate);
              } else if (peakCount == 1) {
              // This is the second peak found, return the time between them
              return i * (1.0 / sampleRate) - peakTime;
              }
              peakCount++;
              }
              lastValue = value;
  }

  // No peaks were found
  return 0.0;
}

void setup() {
  // Initialize the OLED display
  display.begin(SSD1306_SWITCHCAPVCC, 128, 32);

  // Print a message to the display
  display.clearDisplay();
  display.setTextSize(1);
  display.setTextColor(WHITE);
  display.setCursor(0, 0);
  display.println("SpO2 & Heart Rate");
  display.display();
  delay(1000);
}

void loop() {
  // Read the DC signals from the analog inputs
  int redDC = analogRead(redDCPin);
  int irDC = analogRead(irDCPin)

  // Read the AC signals and average over numSamples readings
  float redAC = 0.0;
  float irAC = 0.0;
  for (int i = 0; i < numSamples; i++) {
              redAC += analogRead(redACPin);
              irAC += analogRead(irACPin);
  }
  redAC /= numSamples;
  irAC /= numSamples;

  // Calculate the ratio of AC to DC signals for both red and IR
  float redRatio = redAC / redDC;
  float irRatio = irAC / irDC;

  // Calculate SpO2 using the ratio of red and IR signals
  float ratio = redRatio / irRatio;
  float SpO2 = 110 - 25 * ratio;

  // Calculate heart rate by finding the time between peaks in the AC signals
  float redPeakTime = findPeakTime(redAC);
  float irPeakTime = findPeakTime(irAC);
  float heartRate = 60.0 / (0.5 * (redPeakTime + irPeakTime));

  // Display the results on the OLED display
  display.clearDisplay();
  display.setCursor(0, 0);
  display.print("SpO2: ");
  display.println(SpO2);
  display.print("Heart Rate: ");
  display.println(heartRate);
  display.display();
  delay(1000);
}
```